The effects of asymmetric slip flow between parallel plates of a microchannel under uniform heat flux

Afshin Ahmadi Nadooshan[1]
Faculty of Engineering, Shahrekord University, Shahrekord, Iran
ahmadi@eng.sku.ac.ir

Akram Jahanbakhshi
Faculty of Engineering, Shahrekord University, Shahrekord, Iran
akram.jahanbakhshi@gmail.com

Morteza Bayareh
Faculty of Engineering, Shahrekord University, Shahrekord, Iran
m.bayareh@sku.ac.ir

ABSTRACT

Microchannels have many applications in the field of modern technologies. Today, it is necessary to increase the efficiency of these systems due to the increasing rate of thermal loads. Recent researches have shown that liquid flows in the microchannels depend on their size and surface properties. Consequently, there is no symmetric flow condition in a symmetric geometric channel necessarily. In this study, the effect of slip length on the amount of asymmetric heat transfer in a microchannel is investigated numerically. By calculating the parameters such as Nusselt number and local pressure drop coefficient, it is observed that the asymmetric slip flow affects the flow profile and could lead to a decrease or increase in the heat transfer in the microchannel. According to the results, asymmetric slip flow can lead to a 20-40% reduction or increase in the Nusselt number. The most important point in the design of micro-scale asymmetric cooling systems is the increase of slip length at high temperatures.

Keywords: Asymmetric slip flow, Microchannel, First order slip, Heat transfer.

[1] Corresponding author

INTRODUCTION

In recent years, micro-scale thermal-fluid systems have been widely used in the industries include chemical reaction chambers, fuel cells, computer chip coolers, chemical separators, micro-reactors, etc. Micro-scale flows have differences with the macro-scale ones, such as the existence of a slip surface at the interface of fluid and solid which is referred to slip condition. Most of materials used to fabricate microchips, for example polydimethylsiloxane (PDMS) exhibit hydrophobic or hydrophilic effects due to the slippage of the fluid on its surface. Theas microchips are used for mixing the fluids in the presence or absence of external actuators [1-3]. Thermal filed can be employed to enhance the mixing index in the micromixers.

Hendy et al. [4-5] studied Newtonian flow characteristics in a microchannel using molecular dynamics. The wetting of channel surface affects the amount of wall slip. Qi et al. [6] also studied the effect of surface wetting on the wall slip. They showed that the change in the surface wetting is due to the change in the channel material, which causes the slip length (L_s) to be changed in a flow at a particular Reynolds number (Re). This conclusion has also been reported by other researchers [7-8]. In order to understanding the effects of these characteristics on the flow and thermal parameters that are necessary for the optimal design of these systems, numerous investigations have been carried out numerically and experimentally. In various studies, the effect of different fluids, including Newtonian and non- Newtonian, on these parameters has been studied numerically [9-15]. In these studies, slip and no-slip wall conditions have been investigated and considerable effects of liquids and boundary conditions on heat transfer have been reported. One of these results is the direct relation between L_s and heat transfer. In recent years, rapid technological

developments, especially in the field of electronics, have led to systems with a thermal load of more than 1 kW/cm^2. On the other hand, the reduction of the dimensions of these systems is highly considered by researchers. Therefore, there is still a requirement to study cooling systems and their improvement and pay particular attention to micro-scale systems [16]. Zhang et al. [17] studied natural convection heat transfer in a two-dimensional microchannel at slip flow regime. They found that the viscous heating increases linearly by increasing the Brinkman number and decreases nonlinearly by increasing the Knudsen number. Also, Nusselt number (Nu) of fully developed flow decreases with the Knudsen number. Nikkhah et al. [18] showed that Nu oscillates along the length of the microchannel and increases with Re. Also, Nu increases by increasing the slip coefficient ($\beta = L_s/h$), where H is the channel height, and weight percentage of nanoparticles, which is higher for larger values of Re. Afrand et al. [19] studied the forced convection of FMWNT/water nanofluid in a microchannel under the influence of magnetic field for slip flow regime. They found that the growth of the boundary layer thickness decreases with the Hartmann number. In addition, as the Hartmann number increases (the magnetic field becomes stronger), u_s increases. The effect of gravity on mixed convection in a microchannel was investigated using lattice Boltzmann method (LBM) by Karimipour et al. [20]. They showed that an increase in the Knudsen number leads to an increase in u_s and temperature jump and a reduction in Nu and friction coefficient. The effect of the slip condition on heat transfer and the entropy generation of power-law pressure driven flow in a microchannel under uniform heat flux was investigated by Anand [21]. He showed that, for the same values of β, Nu predicted by the Hatzikiraakos slip law is greater and the average rate of entropy generation is lower than the predicted values by the asymptotic slip law, and this difference increases with β. Sajadifar et al. [22] observed that Nu increases by increasing

the volume fraction and β, which is more significant at high values of Re. Also, for a laminar non-Newtonian fluid flow, higher values of β leads to an increase in the nanofluid velocity along the channel wall.

In the previous studies, the governing slip conditions of the flow have always been symmetric. However, in many cases, especially in electrical systems, the heat flux is applied on cooling systems asymmetrically. Previous numerical simulations have been performed to evaluate the hydrodynamic effects of asymmetry and wall slip on channel flow. For example, Ghosh [23] explored these effects on the stability of a Poiseuille flow in the absence of energy equation. They found that the flow behavior depends on the velocity slip at the upper and lower walls. In the present study, the asymmetric slip flow in a microchannel with parallel surfaces is studied considering the thermal behavior of the fluid flow. Present simulations evaluate the effects of asymmetry and wall slip on heat transfer and pressure drop in the channel flow.

DESCRIPTION OF THE PROBLEM

In this study, the flow of water between two parallel plates is numerically modeled. The channel has a height of 100 μm and a length of 1500 μm. A schematic of the problem is presented in Fig. 1.

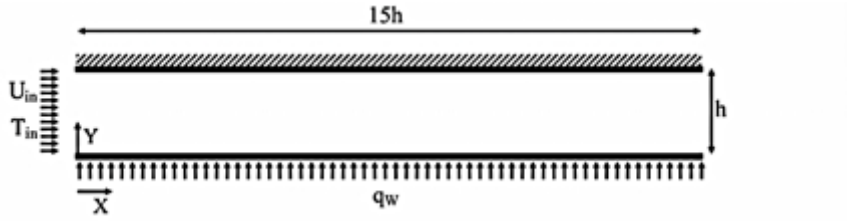

Fig. 1 Schematic of the computational domain.

The flow is assumed to be two-dimensional, steady, incompressible and laminar. Hence, the continuity, momentum and energy equations are as follows, respectively [15, 24]:

$$\nabla.\vec{V} = 0 \tag{1}$$

$$\rho\vec{V}.\nabla\vec{V} = -\nabla \mathrm{p} + \mu\nabla^2\vec{V} \tag{2}$$

$$\rho C_p\vec{V}.\nabla T = k\nabla^2 T \tag{3}$$

where $\vec{V}$ is the velocity vector, p is the pressure, ρ is the density, μ is the dynamic viscosity, C_p is specific heat and *T* is the temperature. The effect of body forces is neglected and fluid properties are assumed to be constant. The flow enters the microchannel with uniform temperature and velocity and is placed under a uniform heat flux of 50,000 W/m^2 applied on the bottom wall. The other wall is assumed to be insulated. The first-order slip boundary condition is used on the walls as follows:

$$\Delta u|_{wall} = L_s \left.\frac{\partial u}{\partial \vec{n}}\right|_{wall} \tag{4}$$

where u is tangential velocity and $\vec{n}$ is normal vector to the wall. L_s is the distance from which the velocity profile becomes zero using extrapolation, in which case the continuity condition is satisfied [25]. The governing equations are solved using a finite volume method based on the SIMPLE algorithm [26-27]. Second order upwind scheme is employed to discretize the governing equations [28]. The convergence criterion is assumed to be 10^{-6}. Several grid resolutions (30×150, 65×300, 130×600, and 185×900) are used to study the grid independency and it is found that the difference between the Nusselt number obtained

using the grid resolutions of 130×600 and 185×900 are negligible. Hence, the grid resolution of 130×600 is used for further simulations.

The following relationships are used to nondimensionalize the equations:

$$Y = \frac{y}{h}, \qquad X = \frac{x}{h}, \qquad \Theta = k\frac{T - T_{inlet}}{hq_w}, \qquad \vec{U} = \frac{\vec{u}}{\vec{U}_{in}},$$

$$f = \frac{-h\left(\partial p / \partial x\right)}{\rho U_{in}^2/2}, \qquad F = \frac{P_{inlet} - P_{outlet}}{\rho U_{in}^2/2}, \qquad Re = \frac{2\rho U_{in} h}{\mu},$$

$$Nu_x = \frac{\mathrm{q_w}\lambda}{\mathrm{k[T_w(x) - T_m}(x)]}, \qquad Nu_{ave} = \frac{1}{L}\int_0^{L=15h} Nu(x)dx,$$

$$T_m = \frac{\int_0^h u(y)T(y)dy}{\int_0^h u(y)dy} \tag{5}$$

VALIDATION

Since the asymmetric heat transfer has not been studied so far, two different studies are used to verify the present simulations. The grid resolution is based on the numerical simulations of Shojaeian et al. [15] who studied symmetric slip boundary condition and asymmetric heat transfer. The fully developed velocity profile for no-slip and symmetric slip conditions are compared with the numerical results obtained by Shojaeian et al. [15] in Fig. 2. This figure shows that the present results are in very good agreement with the ones presented by Shojaeian et al. [15]. To verify the accuracy of the asymmetric slip condition, the present results are compared with the results of Wang [25] who calculated the velocity profile of fully developed flow under asymmetric slip condition analytically. Fig.

3 demonstrates that there is very good agreement between the numerical simulations and analytical results.

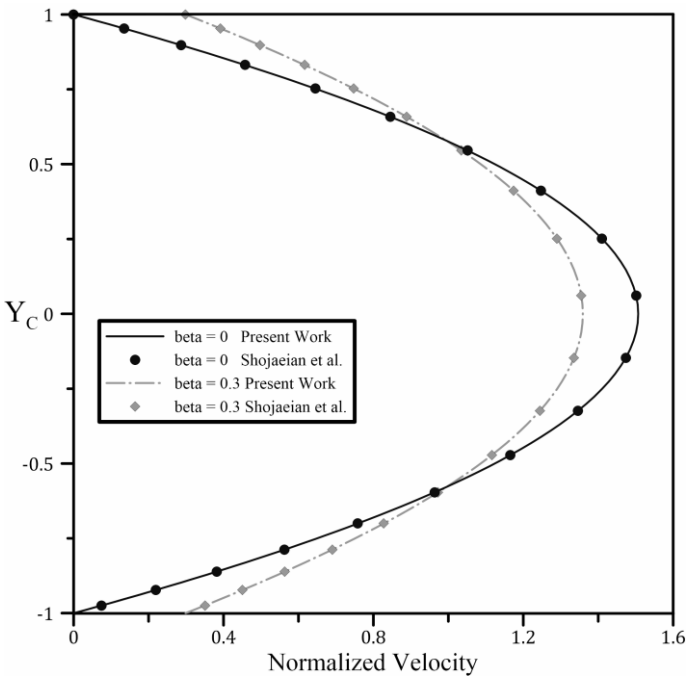

Fig. 2 Validation of velocity profile for symmetric velocity compared to the results of Shojaeian et al. [15].

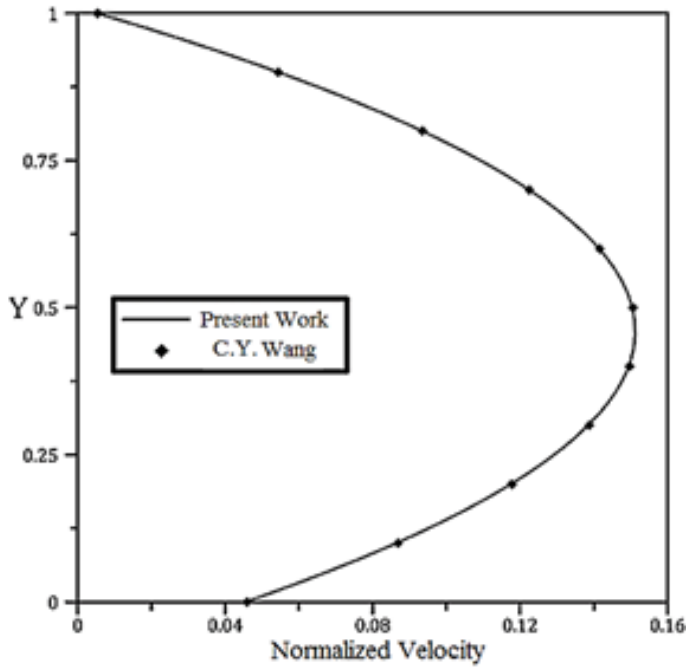

Fig. 3 Validation of velocity profile for asymmetric slip condition compared to the results of Wang [25].

Also, Fig. 4 shows Nu to verify the thermal behavior of the present simulations compared to the results obtained by Shojaeian et al. [15], which shows the adequacy of the present numerical method.

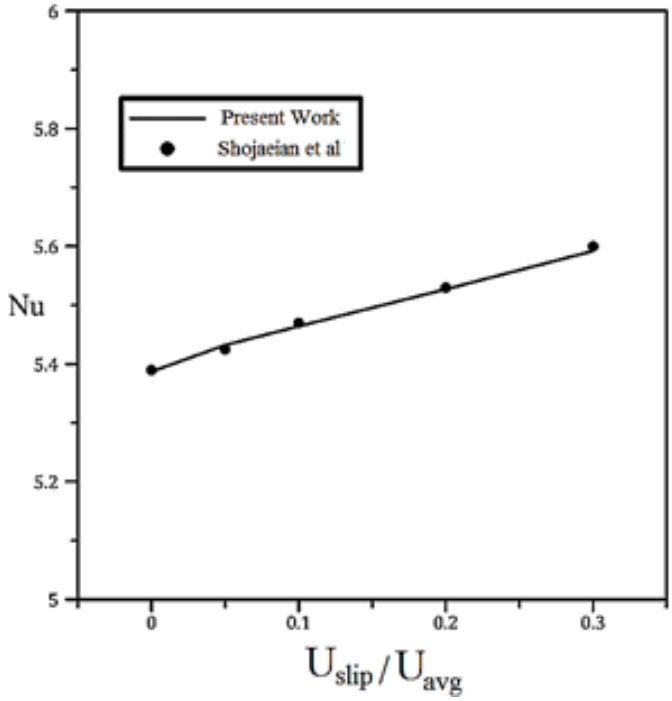

Fig. 4 Nu in terms of dimensionless slip velocity obtained from the present simulations in comparison with the results reported by Shojaeian et al. [15].

RESULTS AND DISCUSSION

In this study, the effect of non-uniformity of channel walls and therefore, the difference in L_s of two walls on thermal and flow field is studied. There are some limitations in the present study. One of them is that the influence of temperature variations on the properties of fluid such as density and viscosity is assumed to be negligible, leading to simpler form of Navier-Stokes equations. Since the imposed heat flux is small, this limitation is valid [21]. Another limitation is that the surface characteristics such as relative roughness are considered to be homogeneous along the channel.

HYDRODYNAMIC POINT OF VIEW

In Fig. 5, the velocity profile is shown at several sections of the channel for Re = 10. This figure shows the bottom wall with β = 0.01 and the top one with different values of β.

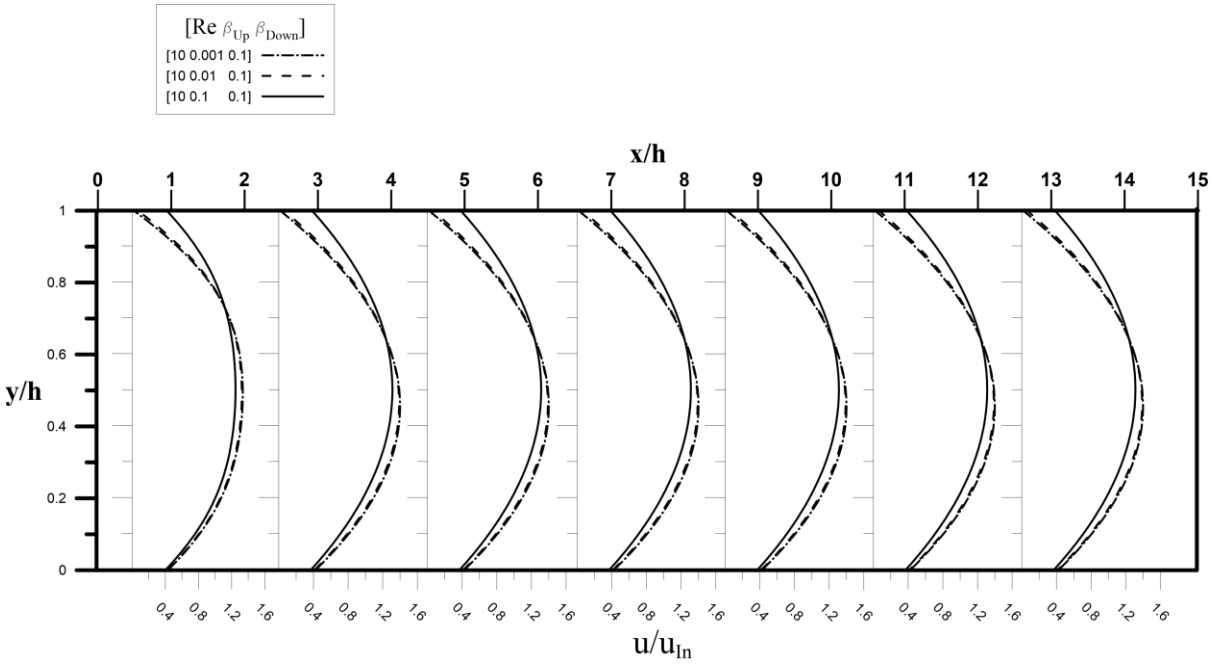

Fig. 5 The velocity profile at different sections of the channel at Re = 10.

According to the figure, the relationship between L_s and the velocity profile is nonlinear. u_s in the range of β = 0.01 and β = 0.001 is not significantly different, but u_s on top wall increases considerably for 0.01 < β < 0.1. Although the slip is constant on the bottom wall, the fluid velocity on the wall slightly increases by decreasing β of the top wall. It should be pointed out that the position of maximum velocity at the cross section changes with β. The point in which the maximum velocity occurs is shifted towards the bottom wall due to a reduction in β. It means that the flow momentum near the bottom wall increases and the flow becomes asymmetry. For example, the maximum velocity for β = 0.001 and 0.1 is 0.44 and 0.5 for Re = 10 and x/h = 7, respectively. As a result, as β decreases, the flow rate increases. It was demonstrated that resistance against the fluid flow decreases when

hydrophobic coating is used on the microchannel walls for the same pressure drop [29]. By keeping constant the top wall slip coefficient and changing β on the bottom wall, the expressed trend is reversed, and this process occurs for the top wall. This symmetrical behavior is shown in Fig. 6 for Re = 100.

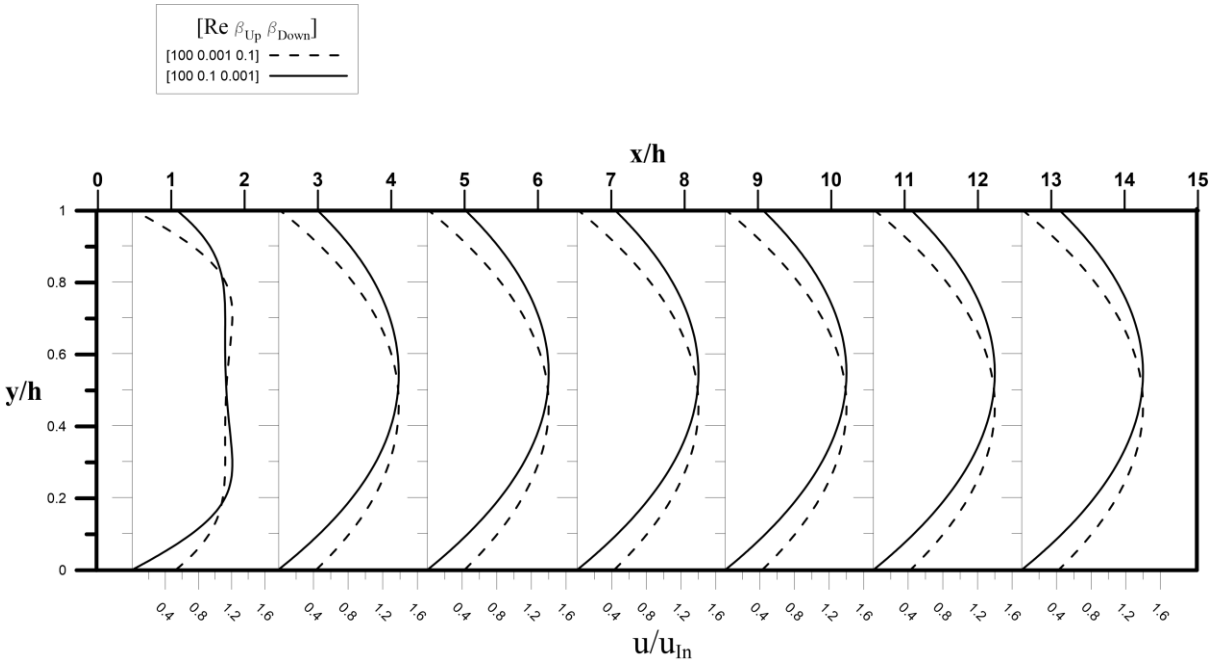

Fig. 6 The velocity profile at different sections of the channel at Re = 100.

Fig. 6 shows the velocity profile at the inlet section. Comparison with the Fig. 5, it can be stated that an increase in the entrance length is due to the increase of Re. The velocity profile is plotted in Fig. 7 for different values of β at Re = 1000. This figure shows that the slip coefficients of β = 0.001 and β = 0.01 on one wall have no significant difference on the velocity profile. But the maximum velocity increases compared to the symmetric slip condition. It is also observed that the fully developed flow does not occur at Re = 1000.

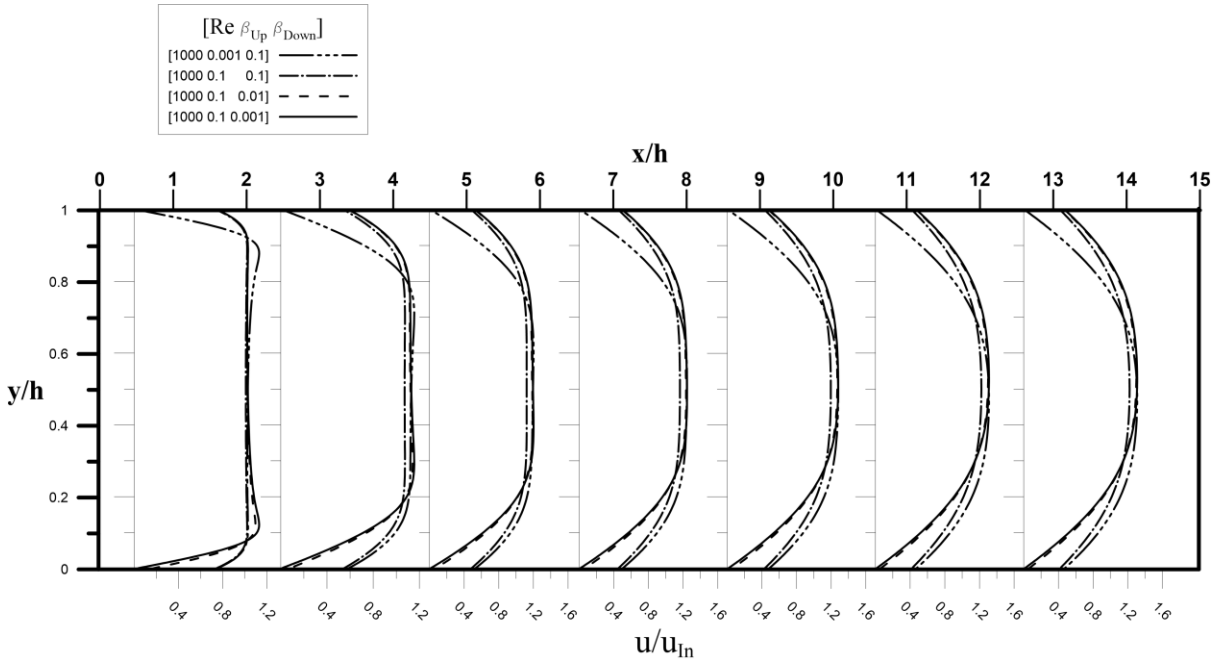

Fig. 7 The velocity profile at different sections of the channel at Re = 1000.

The asymmetric effect of $L_s$on local pressure drop is shown in Figs. 8 and 9 for Re = 10 and 1000, respectively.

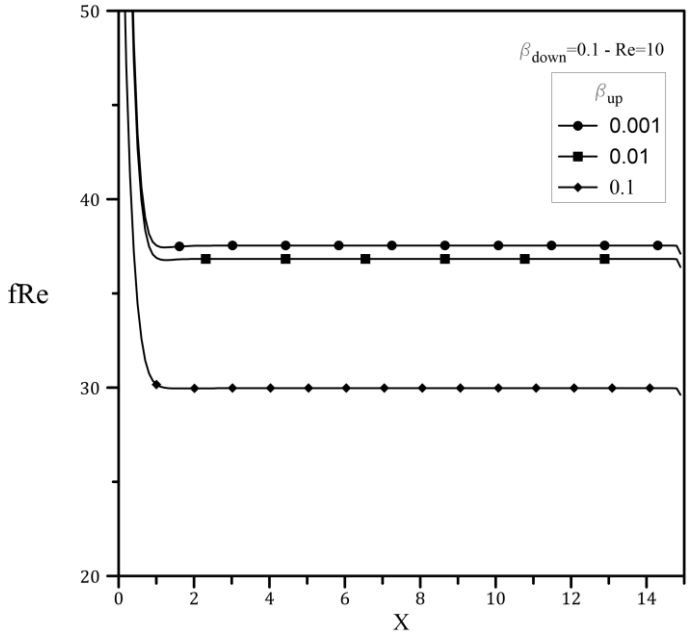

Fig. 8 Local pressure drop in the channel at Re = 10.

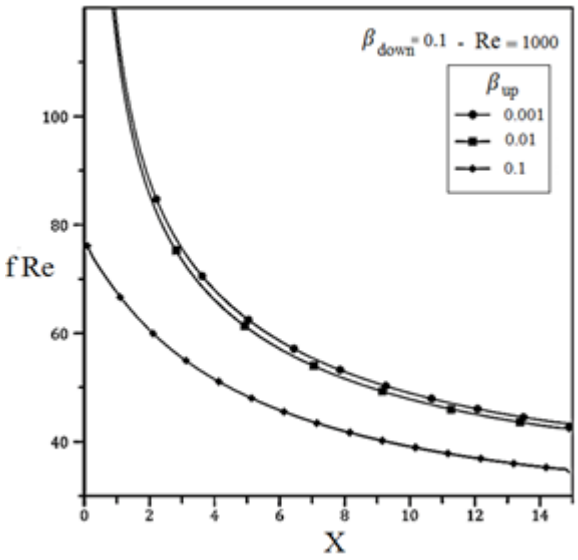

Fig. 9 Local pressure drop in the channel at Re = 1000.

These figures show that the pressure drop increases by decreasing β on a wall. This is due to the increase of wall resistance against the fluid velocity. For example, at Re = 10 and X = 8, f×Re = 37.5, 36.7, and 29.9 for β = 0.001, 0.01, and 0.1, respectively. It is worth noting that the values of f remain constant for X ~ 1.5, indicating that the velocity profile does not change along the channel for Re = 10. However, at Re = 1000 and X = 8, f×Re = 52.9, 51.6, and 41.5 for β = 0.001, 0.01, and 0.1, respectively. The values of local pressure drop increases with Re for a given length of the channel. In addition, the values of pressure drop vary with X. Thus, fully developed flow occurs at Re = 10 in contrast to Re = 1000.

THERMAL POINT OF VIEW

In the previous section, it was observed that by decreasing L_s, the flow tends to move towards the other wall. To observe the effect of this phenomenon on the amount of heat transfer on the hot wall, the temperature profile is plotted at the same sections along

the channel in Fig. 10 for Re = 1000. This figure shows that when the slip on the hot wall is less than the other wall, the fluid temperature in the vicinity of the wall increases.

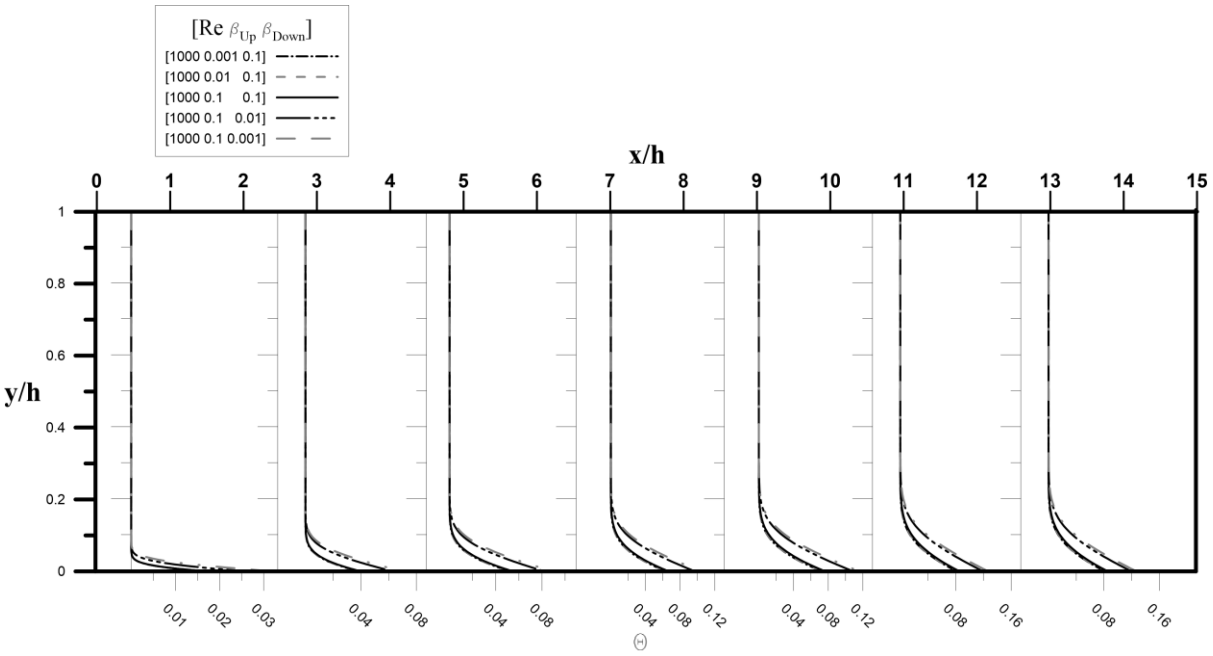

Fig. 10 The temperature profile at different sections of the channel at Re = 1000.

This is due to the reduction in the energy transport capability of the fluid near the hot wall because the heat flux is constant and the reducing effect of the flow rate near the wall is compensated by increasing the fluid temperature in this area. As β increases, the advection in the vicinity of the wall enhances, leading to positive effect on heat transfer rate [15]. This is due to a reduction in the temperature gradient between the fluid and the wall. As Re increases, the effect of slippage increases. Fig. 11 demonstrates that the negative effect of asymmetric slip condition when L_s of the hot wall is less than the other wall is more than its positive effect at a time when L_s of the hot wall is more than the other wall.

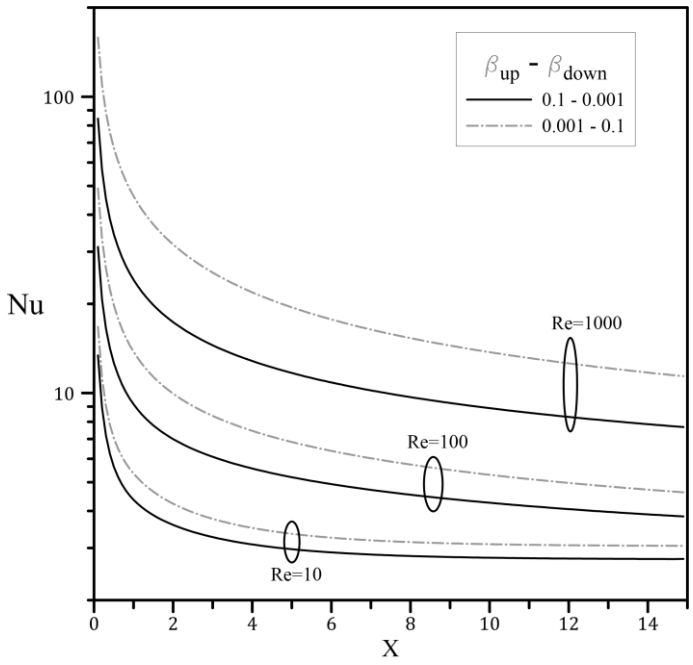

Fig. 11 Nu_x for different asymmetric slip coefficients.

This is due to the change in the velocity profile due to asymmetric slip condition, and the increase in Re also exacerbates the difference, as shown in Fig. 12. This figure shows the local Nusselt number (Nu_x) for three different Reynolds numbers for maximum difference of each condition. This figure also shows that the flow with Re = 100 does not reach thermally fully developed region, even though it reaches hydrodynamic fully developed region.

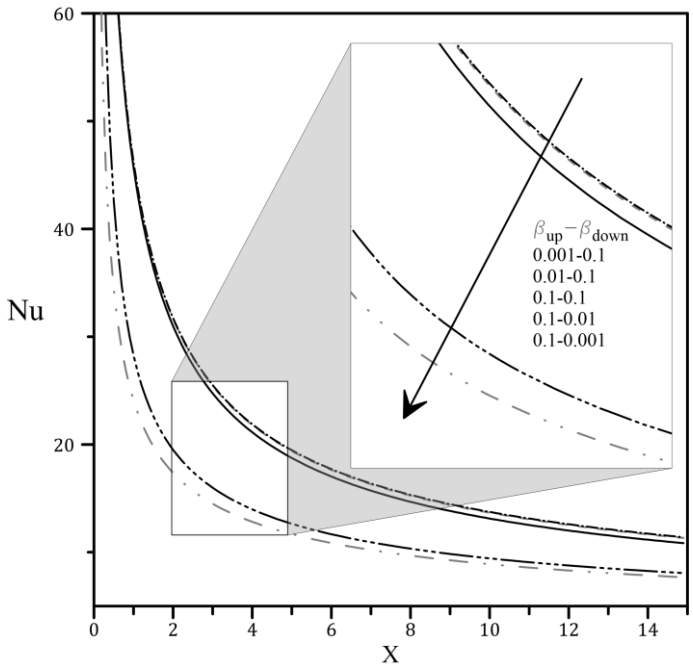

Fig. 12 Nu_x along the channel at Re = 1000.

Finally, for comparing the microchannel cooling performance, the average Nusselt number (Nu_{ave}) and total pressure drop are calculated for different cases. Figs. 13 and 14 show these values for Re = 10 and 1000 and different values of β.

Fig. 13 shows that the difference of 10 and 100 times of L_s between the two walls at Re = 10 leads to an increase in the pressure drop by 24% and 30% as compared to the symmetric condition, respectively.

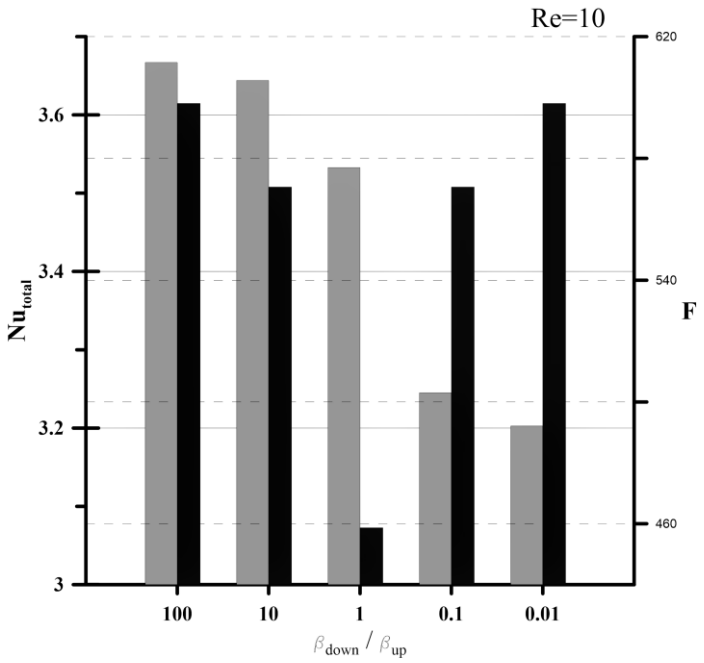

Fig. 13 Nu_{ave} and total pressure drop at Re = 10.

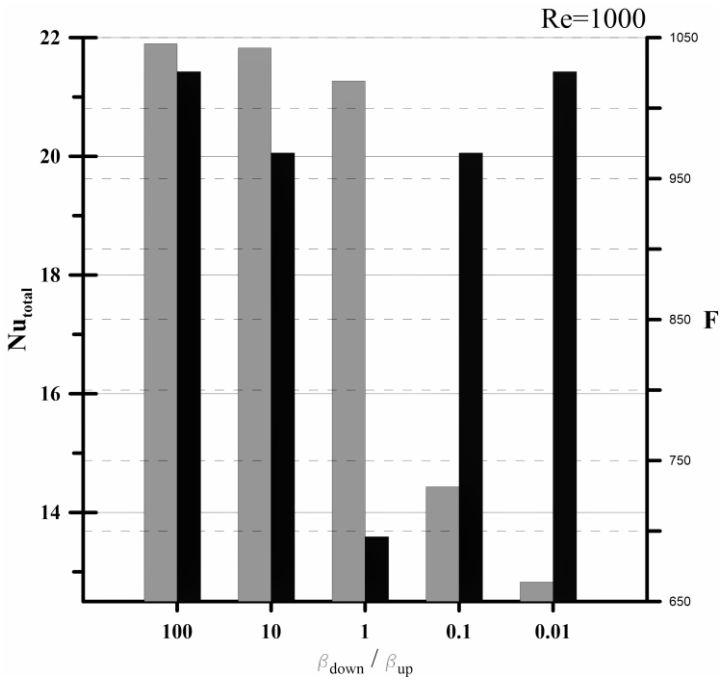

Fig. 14 Nu_{ave} and total pressure drop at Re = 1000.

While the heat transfer rate increases by 3.2 and 3.8 %, respectively, for larger L_s relative to the symmetrical condition. It decreases by 8.2 and 9.3 %, respectively, for smaller L_s of the hot wall relative to the symmetrical condition. These values for Re = 1000 are as follows: the

increase in the pressure drop by 39% and 47%, the increase in Nu by 2.6% and 3% for larger L_s of the hot wall and the decrease in Nu by 32% and 40% for smaller L_s of the hot wall. In Fig. 15, the maximum and minimum values of Nu are presented. This figure shows that the difference in Nu due to the asymmetric slip condition increases with Re, which is roughly exponential.

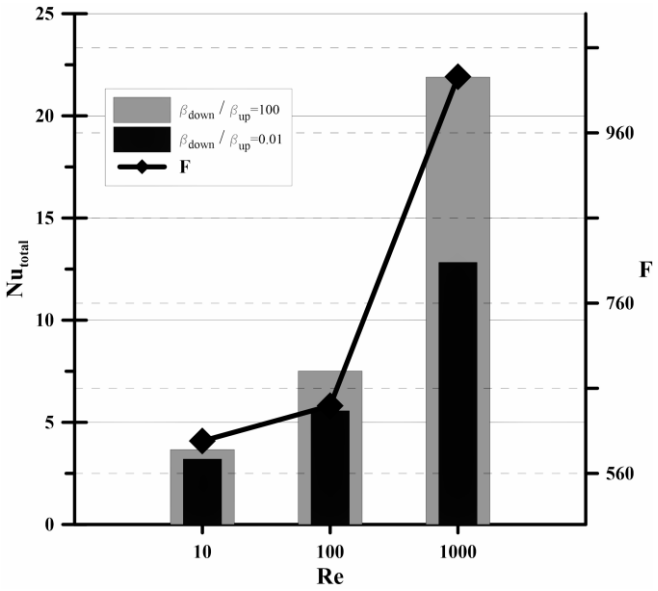

Fig. 15 Nu_{ave} and total pressure drop for different values of Re.

CONCLUSION

Due to the influence of the slippage of fluids on the surface of microchannels used in microfluidic devices, for example micromixers, the asymmetric effect of L_s in a microchannel with parallel surfaces was investigated numerically. The microchannel had an asymmetric uniform heat flux. It was found that the difference in L_s of the walls leads to that the flow moves towards the wall with a greater β. As L_s of a wall decreases, the maximum velocity increases relative to the symmetric condition and its position moves towards the wall with a greater β. Reducing the slip length on the hot wall leads to an increase in the temperature of the fluid near the wall. The results demonstrated that Nu of

the hot wall decreases by decreasing L_s. It slightly increases with a decrease in L_s of the opposite wall. For the design of micro-scale asymmetric cooling systems, the priority is to increase L_s on the hot wall.

Acknowledgment

This work has been financially supported by the research deputy of Shahrekord University.

REFERENCES

[1] Usefian, A., Bayareh, M., Shateri, A., Taheri, N., 2019, "Numerical study of electro-osmotic micro-mixing of Newtonian and non-Newtonian fluids," Journal of the Brazilian Society of Mechanical Sciences and Engineering, **41**(5), P. 238.

[2] Usefian, A., Bayareh, M., 2019, "Numerical and experimental study on mixing performance of a novel electro-osmotic micro-mixer," Meccanica, **54**(8), PP. 1149-1162.

[3] Usefian, A., Bayareh, M., Ahmadi Nadooshan, A., 2019, "Rapid mixing of Newtonian and non-Newtonian fluids in a three-dimensional micro-mixer using non-uniform magnetic field," Journal of Heat and Mass Transfer Research, **6**(1), PP. 55-61.

[4] Hendy, S. C., Jasperse, M., Burnell, J., 2005, "Effect of patterned slip on micro- and nanofluidic flows," Phys. Rev. E - Stat. Nonlinear, Soft Matter Phys., **72**(1), P. 016303.

[5] Hendy, S. C., Lund, N. J., 2007, "Effective slip boundary conditions for flows over nanoscale chemical heterogeneities," Phys. Rev. E - Stat. Nonlinear, Soft Matter Phys., **76**(6), P. 066313.

[6] Qi, H., Liang, A., Jiang, H., Chong, X., Wang, Y., 2018, "Effect of Pipe Surface Wettability on Flow Slip Property," Ind. Eng. Chem. Res., **57**(37), pp. 12543–12550.

[7] Chun, M.-S., Lee, S., 2005, "Flow imaging of dilute colloidal suspension in PDMS-based microfluidic chip using fluorescence microscopy," Colloids Surfaces A Physicochem. Eng. Asp., **267**(1–3), pp. 86–94.

[8] Byun, D., Kim, J., Ko, H. S., Park, H. C., 2008, “Direct measurement of slip flows in superhydrophobic microchannels with transverse grooves,” Phys. Fluids, 20(11), p. 113601.

[9] Tretheway, D. C., Meinhart, C. D., 2004, “A generating mechanism for apparent fluid slip in hydrophobic microchannels,” Phys. Fluids, **16**(5), pp. 1509–1515.

[10] Rosengarten, G., Cooper-White, J., Metcalfe, G., 2006, “Experimental and analytical study of the effect of contact angle on liquid convective heat transfer in microchannels,” Int. J. Heat Mass Transf., **49**(21–22), pp. 4161–4170.

[11] Ngoma, G. D., Erchiqui, F., 2007, “Heat flux and slip effects on liquid flow in a microchannel,” Int. J. Therm. Sci., **46**(11), pp. 1076–1083.

[12] Morini, G. L., 2005, “Viscous heating in liquid flows in micro-channels,” Int. J. Heat Mass Transf., **48**(17), pp. 3637–3647.

[13] Shojaeian, M., Shojaee, M. N., 2013, “Viscous dissipation effect on heat transfer characteristics of mixed electromagnetic/pressure driven liquid flows inside micropumps,” Korean J. Chem. Eng., **30**(4), pp. 823–830.

[14] Shojaeian, M., Koşar, A., 2014, “Convective heat transfer and entropy generation analysis on Newtonian and non-Newtonian fluid flows between parallel-plates under slip boundary conditions,” Int. J. Heat Mass Transf., **70**, pp. 664–673.

[15] Shojaeian, M., Nedaei, M., Yildiz, M., Kosar, A., 2017, “Numerical Heat Transfer and Entropy Analysis on Liquid Slip Flows Through Parallel-Plate Microchannels,” J. Therm. Sci. Eng. Appl., **10**(2), p. 021003.

[16] Kandlikar, S. G., Colin, S., Peles, Y., Pease, R. F., Brandner, J. J., Tuckerman, D. B., 2013, “Heat Transfer in Microchannels—2012 Status and Research Needs,” J. Heat Transfer, **135**(9), p. 091001.

[17] Zhang, T., Jia, L., Yang, L., Jaluria, Y., 2010, “Effect of viscous heating on heat transfer performance in microchannel slip flow region,” International Journal of Heat and Mass Transfer, **53**, pp. 4927–4934.

[18] Nikkhah, Z., Karimipour, A., Safaei, M. R., Forghani-Tehrani, P., Goodarzi, M., Dahari, M., Wongwises, S., 2015, “Forced convective heat transfer of water/functionalizedmulti-walled carbon nanotube nanofluids in a microchannel with oscillating heat flux and slip boundary condition,” International Communications in Heat and Mass Transfer, **68**, pp. 69–77.

[19] Afrand, M., Karimipour, A., Ahmadi Nadooshan, A., Akbari, M., 2016, “The variations of heat transfer and slip velocity of FMWNT-water nano-fluid along the micro-channel in the lack and presenceof a magnetic field,” Physica E, **84**, pP. 474–481.

[20] Karimipour, A., Hossein Nezhad, A., D’Orazio, A., Shirani, E., 2012, “Investigation of the gravity effects on the mixed convection heat transfer in a microchannel using lattice Boltzmann method,” International Journal of Thermal Sciences, **54**, pp. 142-152.

[21] Anand, V., 2014, “Slip law effects on heat transfer and entropy generation of pressure driven flow of a power law fluid in a microchannel under uniform heat flux boundary condition,” Energy, **76**, pp. 716-732.

[22] Sajadifar, S. A., Karimipour, A., Toghraie, D., 2017, “Fluid flow and heat transfer of non-Newtonian nanofluid in a microtube considering slip velocity and temperature jump boundary conditions,” European Journal of Mechanics B/Fluids, **61**, pp. 25–32.

[23] Ghosh, S., 2017, "Relative effects of asymmetry and wall slip on the stability of plane channel flow," Fluids, **2**, p. 66.

[24] Jahanbakhshi, A., Ahmadi Nadooshan, A., Bayareh, M., 2018, “Magnetic field effects on natural convection flow of a non-Newtonian fluid in an L-shaped enclosure,” Journal of Thermal Analysis and Calorimetry, **133**, pp. 1407- 1416.

[25] Wang, C. Y., 2012, “Brief Review of Exact Solutions for Slip-Flow in Ducts and Channels,” J. Fluids Eng., **134**(9), p. 094501.

[26] Shirazi, M., Shateri, A., Bayareh, M., 2018, “Numerical investigation of mixed convection heat transfer of a nanofluid in a circular enclosure with a rotating inner cylinder,” Journal of Thermal Analysis and Calorimetry, **133**(2), pp. 1061–1073.

[27] Bayareh, M., Hajatzadeh Pordanjani, A., Ahmadi Nadooshan, A., Shiryan Dehkordi, K., 2016, “Numerical study of the effects of stator boundary conditions and blade geometry on the efficiency of a scraped surface heat exchanger,” Applied Thermal Engineering, **113**, pp. 1426-1436.

[28] Goodarzi, Z., Ahmadi Nadooshan, A., Bayareh, M., 2018, “Numerical investigation of off-centre binary collision of droplets in a horizontal channel,” Journal of the Brazilian Society of Mechanical Sciences and Engineering, **40**, pp. 1-10.

[29] Duan, Z., Ma, H., He, B., Su, L., Zhang, X., 2019, “Pressure drop of microchannel plate fin heat sinks,” Micromechines, **10**(2), p. 80.